EFFECTS OF THE ELECTRON DISTRIBUTION ON THE EXPANSION OF A COLLISIONLESS PLASMA INTO A BACKGROUND OF LOWER DENSITY

A. V. Mordvinov, V. M. Tomozov,
and V. G. Fainshtein

UDC 533.9.01

Several numerical experiments have been performed [1-3] on the nonlinear flow arising in the one-dimensional expansion of a nonisothermal plasma ($T_e > T_i$) with an initially sharp boundary into a background plasma with substantially lower density ($n_0 \gg n_b$). It has been assumed that the electron velocity distribution is Maxwellian (correspondingly, the energy distribution in the resulting electric field is a Boltzmann one). At the same time, it is known that the nonlinear motion in a plasma may be substantially dependent on the electron distribution $f_e(v)$ [4-6]. In particular, when a collisionless plasma expands into vacuum, the form of that distribution has an appreciable effect on the plasma dynamics, the ion-acceleration performance, and the number of high-energy particles [5, 6]. One expects that the evolution of a density discontinuity for $n_0/n_b \gg 1$ will also be dependent on $f_e(v)$. The relationship is of interest in physics and especially for astrophysical applications.*

Here we give results from a numerical experiment on the propagation of a density discontinuity in a nonisothermal plasma (n_0/n_b = 10-100) with various electron distributions.

Model Choice and Mathematical Formulation. The ion density profile at the start is

$$n_i(x,\ 0) = \begin{cases} n_0, & 0 \leqslant x \leqslant x_0 - d, \\ n_b + \dfrac{x_0 - x}{d}(n_0 - n_b), & x_0 - d < x < x_0, \\ n_b, & x_0 \leqslant x \leqslant L, \end{cases} \tag{1}$$

where n_0 is the unperturbed density in the basic plasma, n_b is the background plasma density, d is the width of the transition layer, and L is the length of the working region.

The dynamics of the ionic component may be described by a kinetic equation for the ion distribution $f_i(u)$ and the self-consistent electric field:

$$\frac{\partial f_i}{\partial t} + u\frac{\partial f_i}{\partial x} + \frac{eE}{M}\frac{\partial f_i}{\partial u} = 0. \tag{2}$$

The characteristic time for plasma parameter change in that case is determined by the motion of the ionic component and is substantially larger than ω_{pe}^{-1} (ω_{pe} is the electron plasma frequency), because the electrons have had time to adjust to the slowly varying potential. The relation between the electron density n_e and the potential φ is given by the equation of state [5]:

$$n_e(\varphi) = \int\limits_{-\infty}^{-\sqrt{-\frac{2e\varphi}{m}}} \left(1 + \frac{2e\varphi}{mv^2}\right)^{-1/2} f_e(v)\,dv + \int\limits_{\sqrt{-\frac{2e\varphi}{m}}}^{+\infty} \left(1 + \frac{2e\varphi}{mv^2}\right)^{-1/2} f_e(v)\,dv. \tag{3}$$

*The expansion of a collisionless plasma in a less dense background is one of the effective mechanisms for the generation of high-energy ions in solar flares. On the assumption that the plasma bunches expand freely (expansion into vacuum) in a solar flare, estimates have been made on the values in [7], while a more detailed analysis on the basis of the latest observations is given in [8, 9].

Irkutsk. Translated from Zhurnal Prikladnoi Mekhaniki i Tekhnicheskoi Fiziki, No. 6, pp. 10-15, November-December, 1985. Original article submitted July 13, 1984.

 0021-8944/85/2606-0764$09.50

We examined the flow of a plasma with $f_e(v)$ in the form

$$f_e(v) = (1-k)f_m(v) + kf_c(v), \tag{4}$$

where

$$f_m = \left(\frac{m}{2\pi T_1}\right)^{1/2} \exp\left(-\frac{mv^2}{2T_1}\right);\ f_c = \frac{3}{4}\left(\frac{m}{2T_2}\right)^{1/2}\left(1+\frac{mv^2}{2T_2}\right)^{-5/2}.$$

In the series of numerical experiments, the temperature ratio T_2/T_1 took the values of 1, 10, and 100. The coefficient k characterizing the proportion of high-energy electrons was taken 0; 0.01; 0.05; 0.1; 0.25; 0.5; 1.

To (2) and (3) we add Poisson's equation

$$\frac{\partial^2\varphi}{\partial x^2} = -4\pi e\left(\int f_i(u)\,du - n_e\right). \tag{5}$$

At the boundaries of the working region, we put

$$\varphi = 0 \ \text{ at } \ x = 0,\ \varphi'_x = 0 \ \text{ at } \ x = L,$$

while the ion temperature for simplicity is taken as zero.

As in [2, 3], the decay of the density discontinuity was examined for various $f_e(v)$ by the large-particle method [10]. The ionic components was represented as a set of model large particles, each of which consisted of a set of real particles having identical speeds. The motion of the large particles in the self-consistent electric field is described by

$$du_j/dt = -e/M\cdot\partial\varphi/\partial x; \tag{6}$$

$$dx_j/dt = u_j,\quad j = 1, 2, \ldots, N, \tag{7}$$

where x_j and u_j are the coordinate and velocity of large ion j, while e and M are the charge and mass of a real ion. Equations (6) and (7) define the characteristics of (2) and in a sense replace the latter.

We reduce (5), (6), and (7) to dimensionless form by the use of the following scales: n_0 density, $r_{D0} = \sqrt{T_1/(4\pi e n_0)}$ length, $\omega_{pi0}^{-1} = \sqrt{M/(4\pi n_0 e^2)}$ time, $c_s = \sqrt{T_1/M}$ velocity, and T_1/e potential. In dimensionless variables we have

$$\partial^2\varphi/\partial x^2 = -(n_i - n_e); \tag{8}$$

$$du_j/dt = -\partial\varphi/\partial x; \tag{9}$$

$$dx_j/dt = u_j, \tag{10}$$

where $n_e(\varphi)$ is defined by (3) with the electron distribution taken in the form of (4).

System (8)-(10) was integrated with respect to time. One time step included solving the boundary-value problem for Poisson's equation (8) and numerical integration of the equations of motion for all the model particles. In solving that boundary-value problem, we used a quasilinearization [11]. The equations of motion were integrated numerically by a difference scheme involving restepping [12].

The calculations were performed with a BÉSM-6 computer. The working region had a length L = 200-250. The size of a dense-bunch region was x − d = 30-50, while the width of the transitional region was d = 1.5. The equations of motion were integrated numerically until the negative-pressure wave reached the left-hand boundary. The number N of model particles characterizes the accuracy and was 4500-5000, with up to 200 particles per cell in the main plasma.

To check the method, the scheme was applied to the expansion of a collisionless plasma into vacuum, and the results were compared with those of [13]. Although the above boundary condition at the right-hand boundary is somewhat incorrect for that case, good agreement was obtained with the results of [13] up to $t \le 25$-30. Also, the calculations for $n_0/n_b = 3$, $f_e(v) = f_m$ were compared with those of [2]. There is a minor difference between the calculated velocity profiles because it was assumed in [2] that $T_i \neq 0$.

Results. The choice of $f_e(v)$ restricted the range of possible new effects and the quantitative differences from the case of a Maxwellian distribution. On the other hand, the choice of $f_e(v)$ in the form of (4) was not accidental; $f_e(v) = f_c$ becomes a power-law distribution for $k = 1$ and that distribution has been used [6] in a numerical study of the expansion of a collisionless plasma into vacuum, where a comparison was made with a Maxwellian $f_e(v)$. It is therefore of interest to establish how the results are altered as n_b/n_0 increases with otherwise equal conditions ($n_b/n_0 = 0$ for expansion into vacuum). On the other hand, some of the electrons in the corona region in a solar flare are heated to high temperatures, and they have closely a power-law distribution at high energies, where the exponent may be compared with the selected value $\alpha = 5/2$. Therefore, calculations with $f_e(v)$ in the form of (4) can be used to analyze ion acceleration in solar flares for plasma expansion into a plasma.

Parts a-c of Figs. 1 and 2 correspondingly show the ion-density profile $n_i(x)$, the velocity profile $u(x)$, and the potential $\varphi(x)$ for various instants for $n_0/n_b = 50$ for $k = 0$ (Maxwellian distribution) and $k = 1$ (power law with the same electron temperature as for $k = 0$). Figures 1 and 2 show for $f_e = f_m$ and f_c correspondingly that the results do not show major qualitative changes with the form of the distribution and agree with the results of [1-3]. The decay of the density discontinuity begins with the motion of the ions to the right. As in the expansion of a collisionless plasma into vacuum [5, 6], a steep leading edge is formed on the density profile. In the present case, its width is finite at a few times the Debye radius r_{D0}. At the same time, the ions in the background plasma move because the electrons from the region with elevated plasma concentration penetrate far beyond the front into the background plasma and produce an electric field there. A negative-pressure wave moves to the left from the original boundary of the dense bunch. Up to $t \leq 5$, the plasma flow differs little from that on expansion into vacuum. At $t > 5$, the speed of the front is almost unaltered, and the front rapidly overturns. Groups of ions with speed greater than that of the front run ahead of it to form a precursor, which contains not only ions derived from the initial dense bunch but also background ions that have been reflected from the moving potential barrier, which is steep in the front region. It has been shown [1, 3] that this effect occurs not with any density difference but only for $n_0/n_b > (n_0/n_b)_{cr}$. For example, according to [1], $(n_0/n_b)_{cr} = 5$ for $T_i/T_e = 0$. For $n_0/n_b < (n_0/n_b)_{cr}$, oscillations occur on the profiles for n_i, u, and φ, which are similar to those in laminar waves [2, 14]. Oscillations occur also for $n_0/n_b > (n_0/n_b)_{cr}$, but their amplitude decreases as n_0/n_b increases. If n_0/n_b exceeds the critical value by only a little, the front reversal is of pulsating character. The particle ejection becomes continuous as n_0/n_b increases (Figs. 1 and 2).

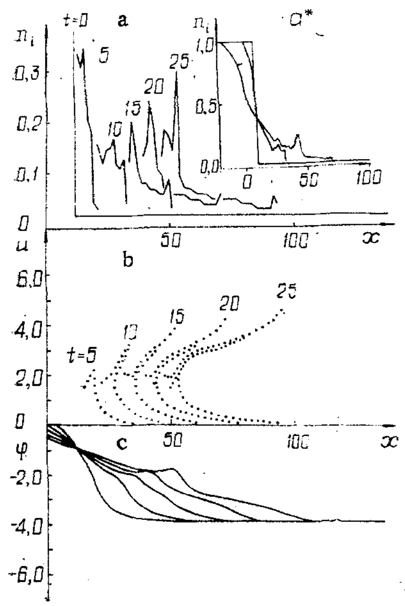

Fig. 1

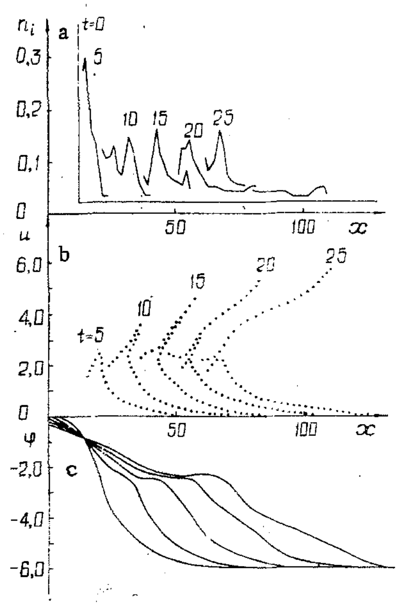

Fig. 2

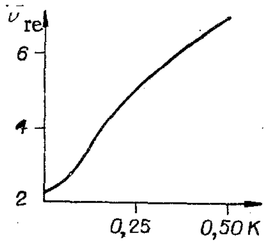

Fig. 3

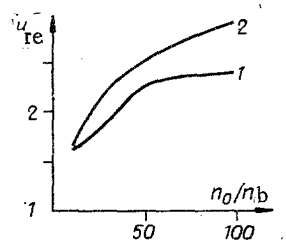

Fig. 4

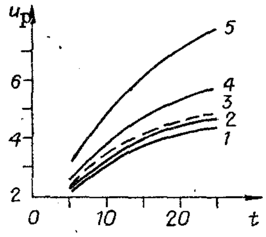

Fig. 5

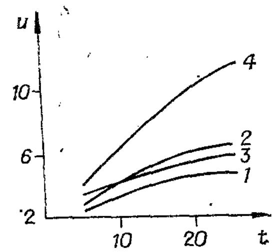

Fig. 6

The electron distribution begins to produce an effect at $n_0/n_b \sim 10$ and subsequently the effects become more pronounced. If the distribution differs from Maxwellian, the spatial scales of certain characteristics increase: front width, electric-field penetration length, and the widths of the plateaux behind the front in the $u(x)$ and $\varphi(x)$ distributions (Fig. 1). This evidently occurs because a power-law distribution decreases much more slowly than a Maxwellian one as the velocity increases. The form of the distribution also influences the speed of the wave at which the overturning occurs (by wave speed is meant the velocity of the ions at the crest of the front). Figure 3 shows the dependence of u_{re} for this reversal on k for $T_2/T_1 = 10$, $t \approx 5$, $n_0/n_b = 50$. Also, u_{re} is appreciably dependent on the initial n_0/n_b (Fig. 4, where $t \approx 5$ and curves 1 and 2 correspond to $f_e(v) = f_m$ and f_c). The data on $n_i(x, t)$, $u(x, t)$ imply that the instant when the front reversal occurs for a given $f_e(v)$ is only slightly dependent on the density difference and is $t_{re} \sim 5$-5.5. At the same time, the spatial scales on which the characteristic features of $n_i(x, t)$, $u(x, t)$, $\varphi(x, t)$ for $t > t_{re}$ increase as n_0/n_b increases, as applies in particular to the formation of plateaux behind the shock-wave front on the $u(x, t)$, $\varphi(x, t)$ profiles and also in the precursor region.

As regards the precursor dynamics, we note that the ions in it continue to be accelerated during the advance into the background plasma (Figs. 1 and 2), which is particularly important for a space (solar) plasma, where they may be major ion acceleration effects as the plasma bunches expand. The reason for the acceleration in the bunches forming the precursor is the same as for the particles in the background plasma ahead of the wave: extensive electric-field penetration into the background plasma. Figure 5 shows the dependence of the speed of the precursor front on time for various $f_e(v)$ for $n_0/n_b = 50$ (curves 1, 2, 4, and 5 correspond to k = 0; 0.01; 0.05; 0.1 for $T_2/T_1 = 10$, while curve 3 corresponds to k = 0.01 for $T_2/T_1 = 100$). Figure 6 shows the analogous curves 1 and 2 for Maxwellian and power-law distributions with identical temperatures $T_1 = T_2$. For comparison, Fig. 6 shows the dependence of the front speed on time for a plasma expanding into vacuum [6] with $f_e = f_m$ and f_c (curves 3 and 4). Figures 5 and 6 indicate the effects of $f_e(v)$ on the precursor motion. A qualitative conclusion can be drawn from these graphs that is analogous to the conclusion for a plasma expanding into vacuum: if the distribution is rich in hot electrons, the ion acceleration is increased. The proportion of fast ions in the precursor is also dependent on the form of $f_e(v)$. At the crest of the precursor front, the ion concentration is higher for a Maxwellian distribution, whereas behind the front, the fast-particle concentration is higher for $f_e(v) = f_c$ than for $f_e(v) = f_m$.

Therefore, the calculations show that the form of the electron distribution has an appreciable effect on the plasma dynamics on expansion into a background plasma of lower density for $n_0/n_b > 10$. This effect for the $f_e(v)$ examined makes itself felt primary in quantitative differences in certain characteristics. The hot tails occurring on the distribution in certain cases or the transition to slow fall at high speeds in $f_e(v)$ emphasizes major characteristics of the nonlinear flow such as the front reversal rate, the speed of the precursor, and the relative fast-particle concentration in the precursor. At the same time, there are increases in the spatial scales of certain features on the $n_i(x)$, $u(x)$, $\varphi(x)$ profiles, while the spatial oscillations in the wave amplitude are smoothed out.

We are indebted to V. M. Bardakov for fruitful discussions.

LITERATURE CITED

1. P. H. Sakanaka, C. K. Chu, and T. C. Marshall, "Formation of ion collisionless shocks," Phys. Fluids, 14, No. 3 (1971).
2. R. J. Mason, "Computer simulation of ion-acoustic shocks: the diaphragm problem," Phys. Fluids, 14, No. 9 (1971).
3. Yu. A. Berezin and V. A. Vshivkov, "Wave processes in a nonisothermal plasma," Zh. Prikl. Mekh. Tekh. Fiz., No. 1 (1973).
4. I. A. Akhiezer and A. E. Borovik, "Nonlinear motion in a plasma with an arbitrary electron-velocity distribution," Zh. Eksp. Teor. Fiz., 51, No. 4 (1966).
5. A. V. Gurevich and L. P. Pitaevskii, "Nonlinear dynamics of low-density plasma and ionospheric aerodynamics," in: Aspects of Plasma Theory [in Russian], No. 10, Atomizdat, Moscow (1980).
6. A. V. Gurevich and A. P. Meshcherkin, "Ion acceleration in an expanding plasma," Zh. Eksp. Teor. Fiz., 80, No. 5 (1981).
7. A. V. Gurevich, L. V. Pariiskaya, and L. P. Pitaevskii, "Ion acceleration on the expansion of a low-density plasma," Zh. Eksp. Teor. Fiz., 63, No. 2 (1972).
8. V. V. Zaitsev, "Some aspects of the dynamics and radio emission of flare loops," Proceedings of the 12th Leningrad Seminar on Space Physics [in Russian], LIYaF, Leningrad (1982).
9. V. G. Eselevich, V. M. Tomozov, and V. G. Fainshtein, "A possible mechanism for ion acceleration in solar flares," Papers at the CAPG Seminar on Solar-Flare Theory [in Russian], Riga (1982).
10. Yu. A. Berezin and V. A. Vshivkov, The Particle Method in Low-Density Plasma Dynamics [in Russian], Nauka, Novosibirsk (1980).
11. R. E. Bellman and R. Kalaba, Quasilinearization and Nonlinear Boundary-Value Problems [Russian translation], Mir, Moscow (1968).
12. D. E. Potter, Computational Physics, Wiley (1973).
13. J. W. Crow, P. L. Auer, and J. E. Allen, "The expansion of a plasma into a vacuum," J. Plasma Phys., 14, Part 1 (1975).
14. R. Z. Sagdeev, "Collective processes and shock waves in low-density plasmas," in: Aspects of Plasma Theory [in Russian], No. 4, Atomizdat, Moscow (1964).